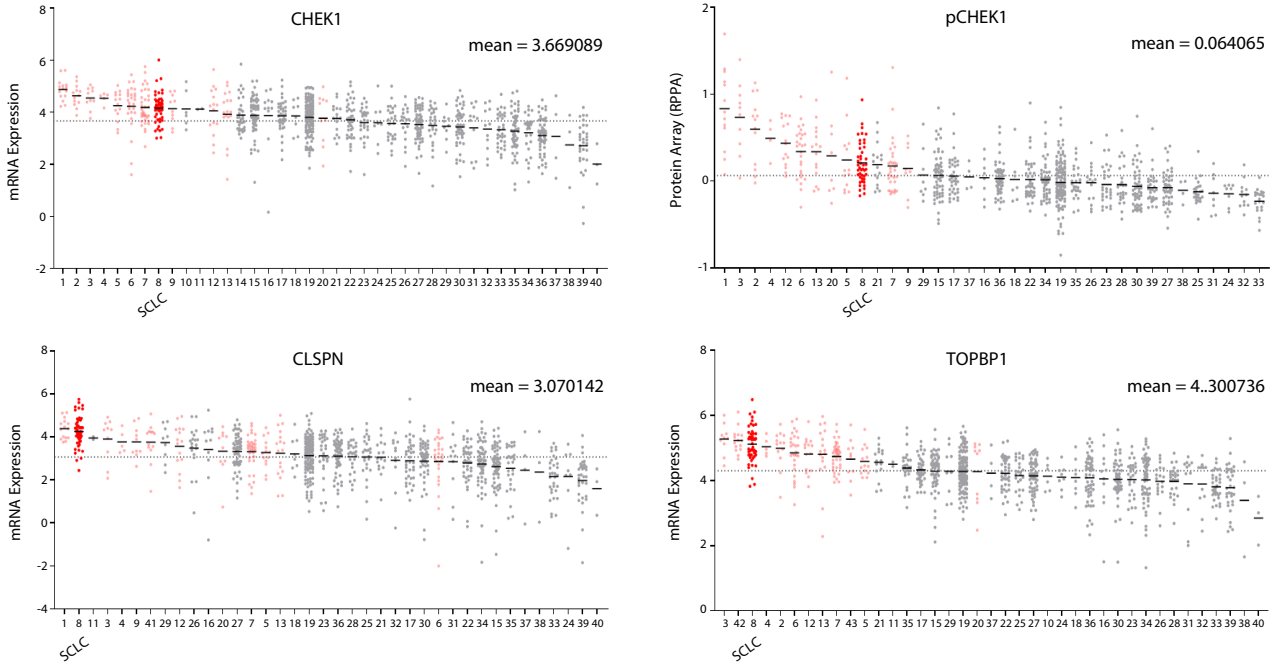


# Figure S1

A



1 T-cell ALL	6 Mult. Myeloma	11 Meningioma	16 Ewing Sarc.	21 Neuroblastoma	26 Soft tissue	32 Thyroid	38 Chondrosarcoma
2 B-cell ALL	7 AML	12 B-cell Lymph. (other)	17 Stomach	22 Pancreas	27 Glioma	33 Kidney	39 Upper aerodigestive
3 Burkitt Lymph.	8 SCLC	13 DLBCL	18 Prostate	23 Endometrium	28 Liver	34 Breast	40 Giant cell tumor
4 Leukemia (other)	9 T-cell Lymph. (other)	14 NA	19 NSCLC	24 Bile duct	29 Osteosarcoma	35 Esophagus	41 B-cell Lymph.
5 CML	10 other	15 Colorectal	20 Lymph. (Hodgkin)	25 Urinary tract	30 Ovary	36 Melanoma	42 T-cell Leuk.
					31 Mesothelioma	37 Medulloblastoma	43 T-cell Lymph.

B

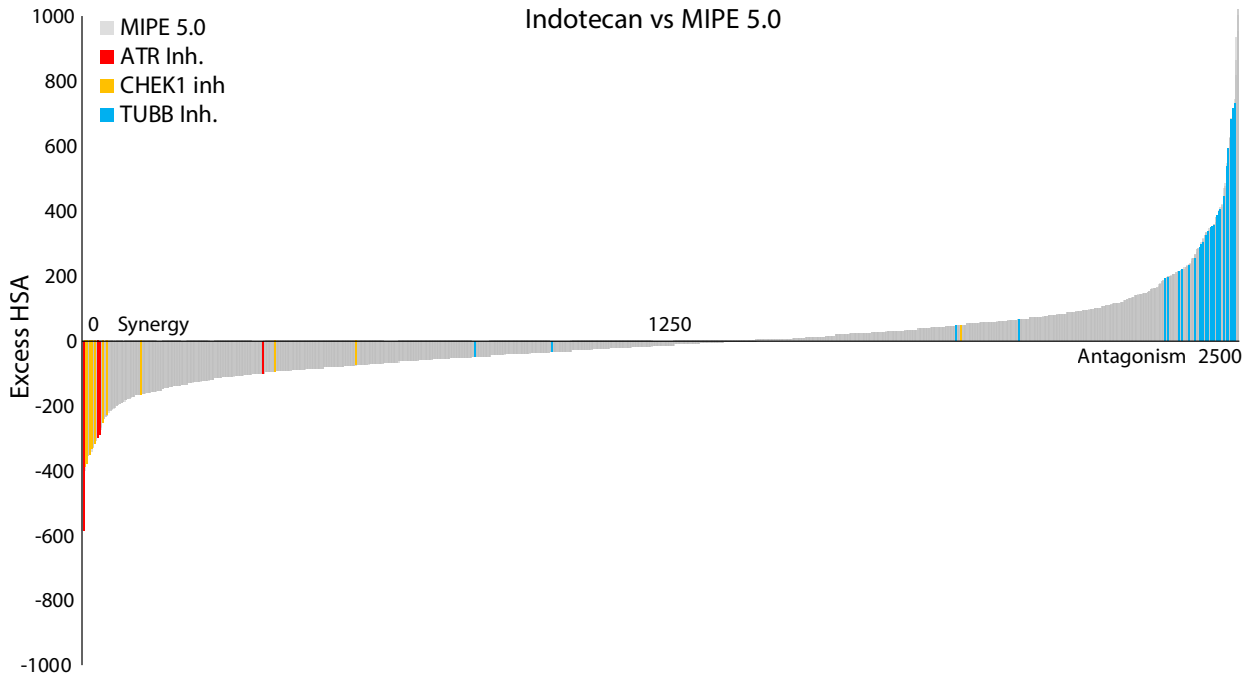
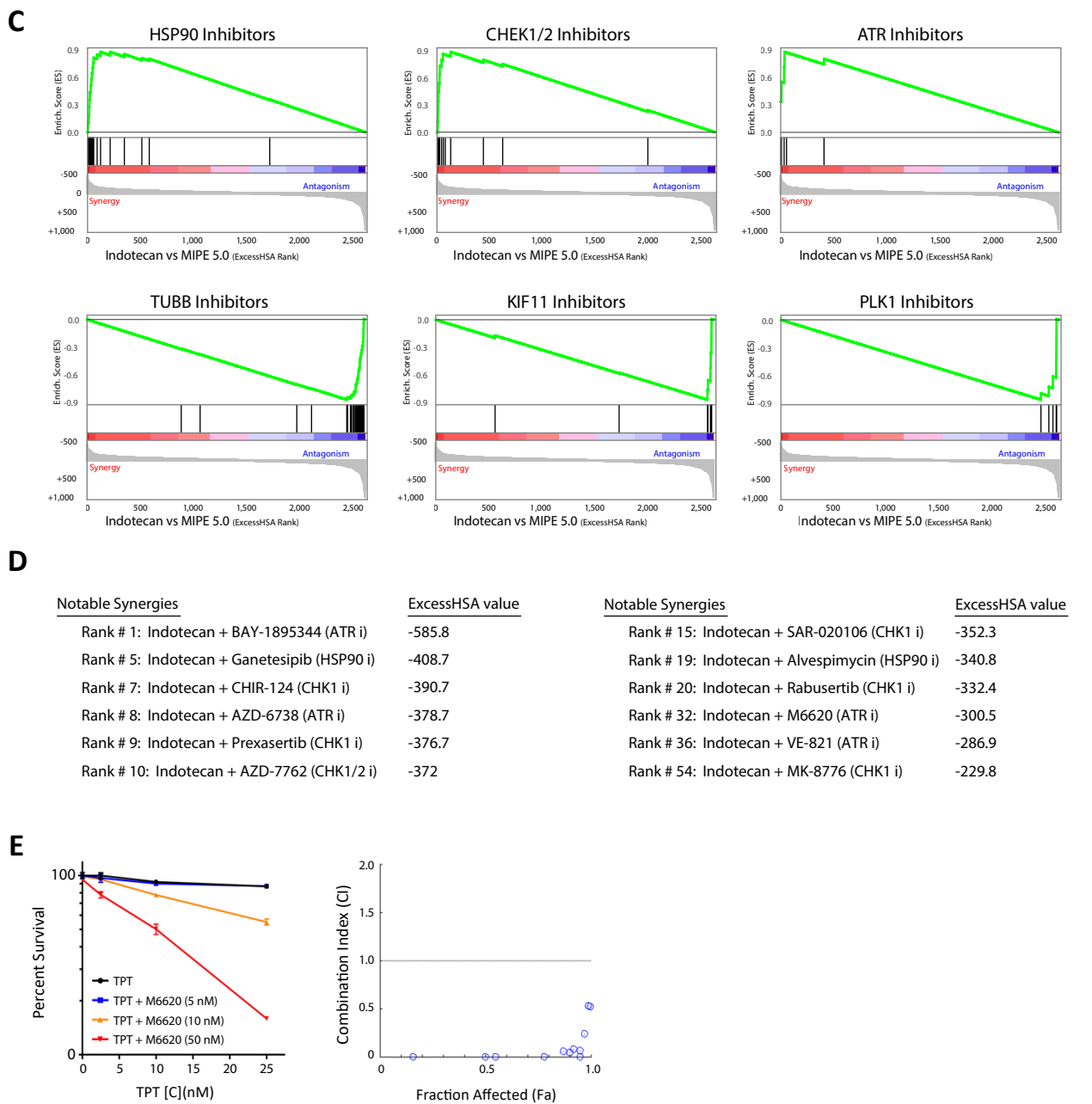


Figure S1 (cont.)



**Figure S1: Combinatorial activity of agents targeting replication stress in SCLC cell lines, related to Figure 1. A)** CHK1, CLSPN, and TOPBP1 mRNA expression and phosphoCHK1 in the CCLE dataset. Red dots and light pink dots indicate small cell lung cancer and hematopoietic malignancy cell lines, respectively. **B)** Ranking of synergy and antagonism of 2480 agents in the MIPE 5.0 library of approved and investigational drugs based on the Excess HSA metric. Prominent mechanistic classes including ATR, CHK1 and tubulin inhibitors are highlighted. **C)** Drug target enrichment analysis (DTEA) plots of the indotecan drug-combination screen highlighting synergy or antagonism enrichments for key drug classes including HSP90, CHK1, ATR, tubulin, KIF11 and PLK inhibitors. **D)** Examples and rankings of notable synergistic indotecan + drug combinations. **E)** Evaluation of H446 cell survival (mean +/- standard deviation, n = 3) following exposure to topotecan and M6620 using fixed ratio dosing and assessment of the combination index (CI) and fraction affected (Fa) for the combination

# Figure S2

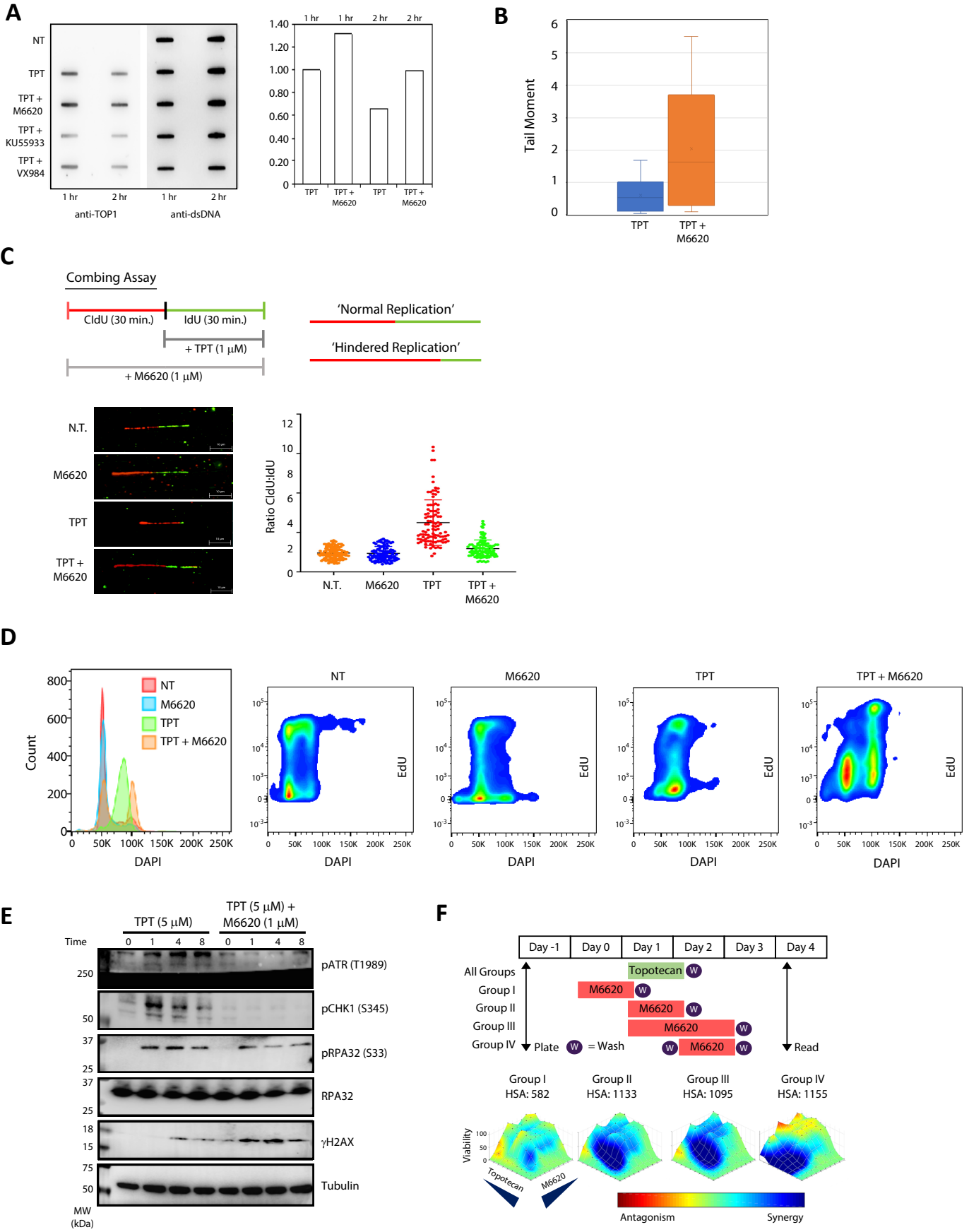
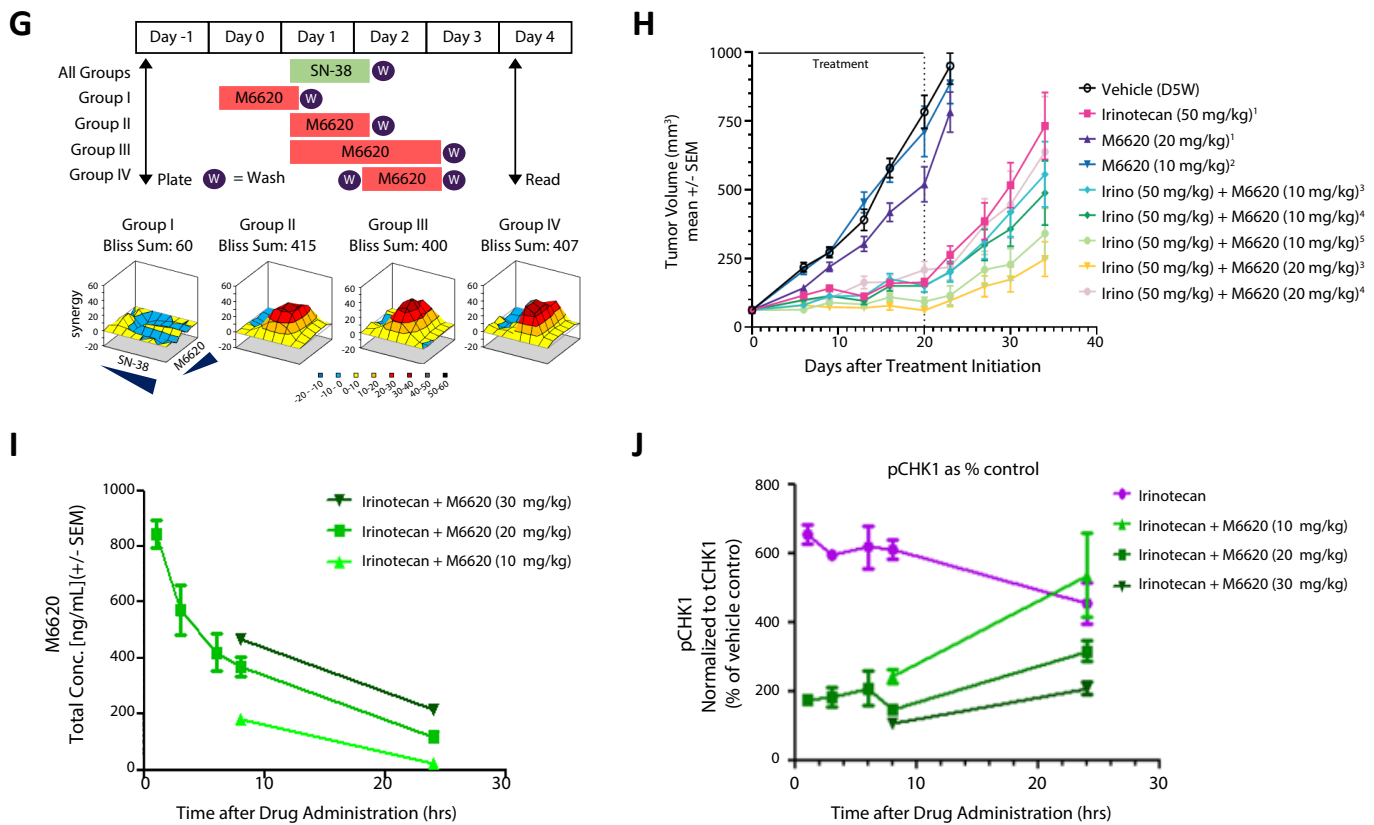


Figure S2 (cont.)

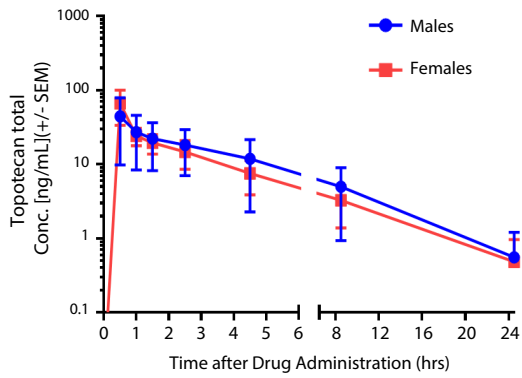


**Figure S2: In vitro and in vivo synergy, mechanistic basis, pharmacokinetic and pharmacodynamic evaluations of the combination of ATR and TOP1 inhibition, related to Figure 2. A)** Evaluation of TOP1 DNA-protein crosslinks (TOP1-DPCs) following exposure to topotecan and M6620. **B)** Quantitation of Comet Assay (single cell gel electrophoresis) demonstrating the increased DNA strand breaks caused by the co-administration of topotecan and M6620. Top and bottom of the boxes are maximum and minimum values, middle line is median and asterisk is mean. Whiskers are upper and lower quartiles. **C)** Schematic illustrating the combing assay (spatiotemporal analysis of DNA replication) for the detection of replication stress and specified imaging outcomes, highlighting the re-establishment of normal replication when M6620 is added to topotecan in the SCLC cell model H209. **D)** Cell cycle evaluation following exposure to topotecan, M6620 or the combination of these agents as flow cytometry and FACS analysis. **E)** Western blot analysis of pCHK1, pRPA and  $\gamma$ H2AX with topotecan and the combination of topotecan + M6642 across three time points (1, 4 and 8 hours). **F)** Cell viability with topotecan and M6620 across different treatment schedules in the SCLC cell line H446. Pre-administration of M6620 followed by topotecan does not yield a synergistic effect on cell viability, while pre-administration of topotecan followed by M6620 and co-administration of these drugs creates a synergistic effect. Group I: M6620 for 24 hours followed by 24 hours of topotecan; Group II: concurrent M6620 and topotecan (24 hours); Group III: concurrent M6620 and topotecan (24 hours) followed by an additional 24 hours of M6620; Group IV: topotecan for 24 hours followed by 24 hours of M6620.

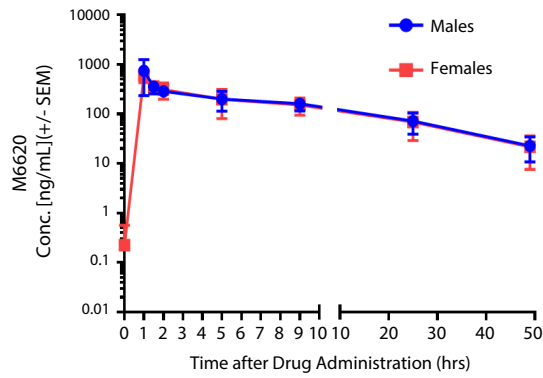
**G)** Cell viability with SN-38 and M6620 across different treatment schedules in the colorectal cancer cell line HT-29. Pre-administration of M6620 followed by SN-38 does not yield a synergistic effect on cell viability, while pre-administration of SN-38 followed by M6620 and co-administration of these drugs creates a synergistic effect. Group I: M6620 for 24 hours followed by 24 hours of SN-38; Group II: concurrent M6620 and SN-38 (24 hours); Group III: concurrent M6620 and SN-38 (24 hours) followed by an additional 24 hours of M6620; Group IV: SN-38 for 24 hours followed by 24 hours of M6620. **H)** Xenograft from human colorectal adenocarcinoma model (Colo205) showing the schedule-dependent effect of irinotecan and M6620. Dosing schedule #1: single agent treatment on day 0; #2: single agent treatment on days 0 and 1; #3: irinotecan day 0 + M6620 day 0; #4: irinotecan day 0 + M6620 day 1; #5: irinotecan day 0 + M6620 days 0 and 1. **I)** Pharmacokinetics of M6620 in tumor bearing mice (HSD athymic) following administration of irinotecan (50 mg/kg) with three different doses of M6620 (10, 20 and 30 mg/kg). **J)** Pharmacodynamic evaluation of phosphoCHK1 (normalized to total CHK1) in tumor bearing mice (HSD athymic) following administration of irinotecan (50 mg/kg) and the combination of irinotecan with three different doses of M6620 (10, 20 and 30 mg/kg).

Figure S3

**A**



**B**

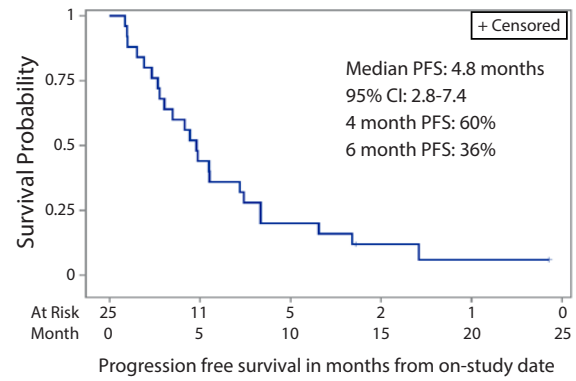


**C**

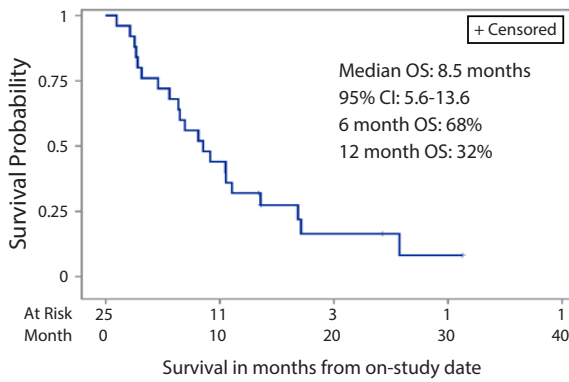
Topotecan and M6620 pharmacokinetic parameters

Parameter	Mean	%CV
<b>Topotecan</b>		
Cmax (ng/mL)	55.2	64.10%
AUCinf (hr*ng/mL)	143.3	59.70%
T1/2 (hr)	4.14	12.90%
Vd (L)	102.8	41.20%
CL (L/hr)	20.7	38.60%
<b>M6620</b>		
Cmax (ng/mL)	663.7	57.20%
AUCinf (hr*ng/mL)	5320	33.30%
T1/2 (hr)	13.4	20.10%
Vd (L)	1509	42.60%
CL (L/hr)	84	33.60%

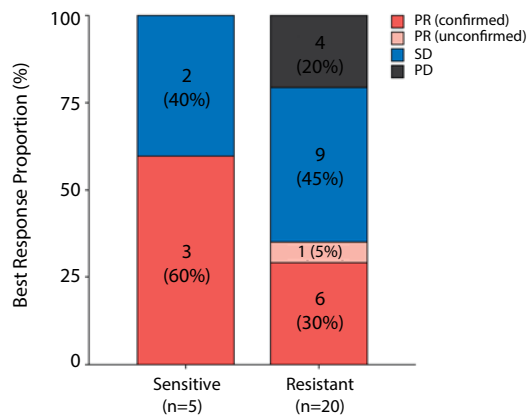
**D**



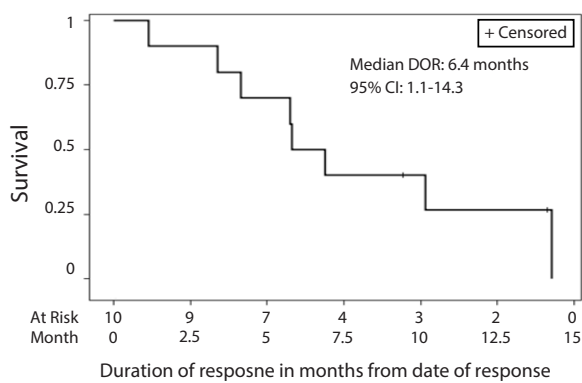
**E**



**F**



**G**



**H**

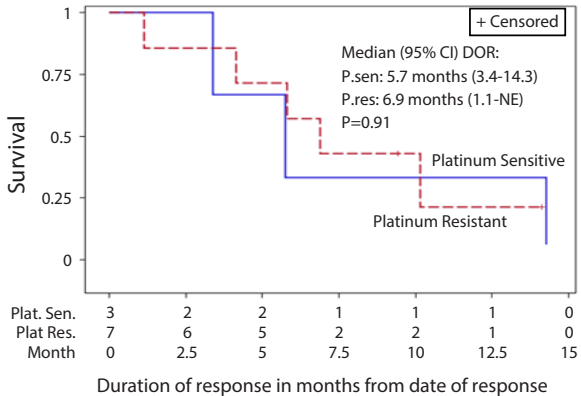
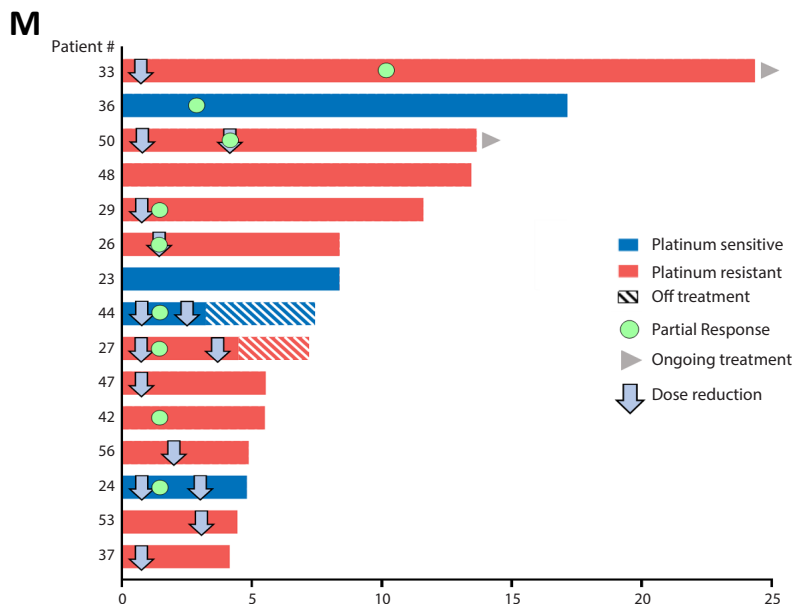
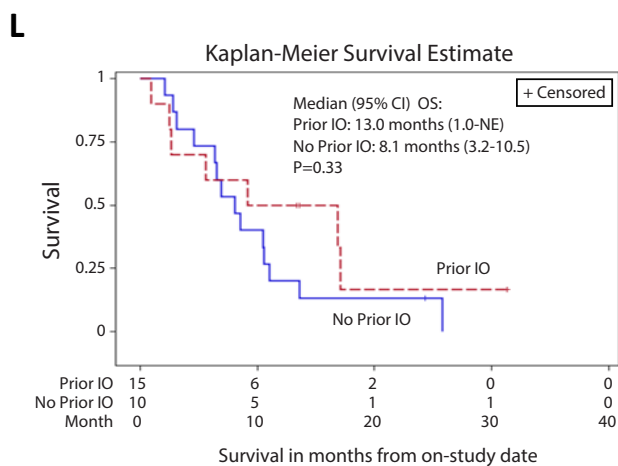
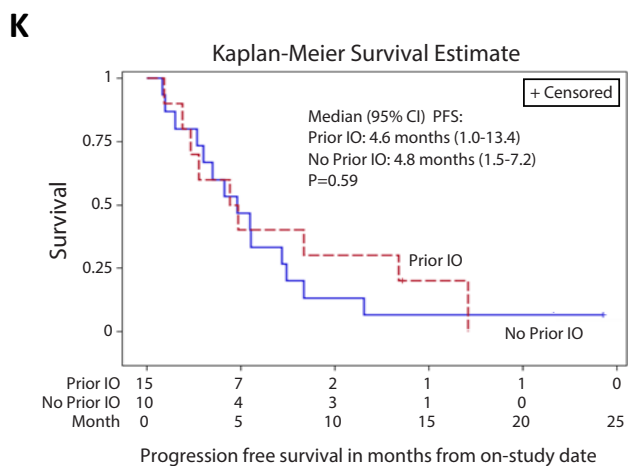
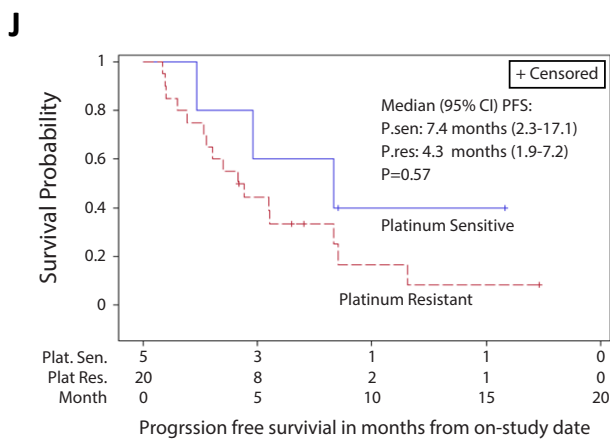
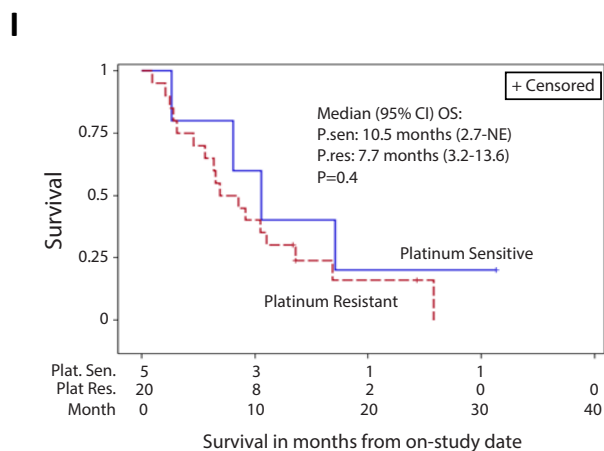


Figure S3 (cont.)

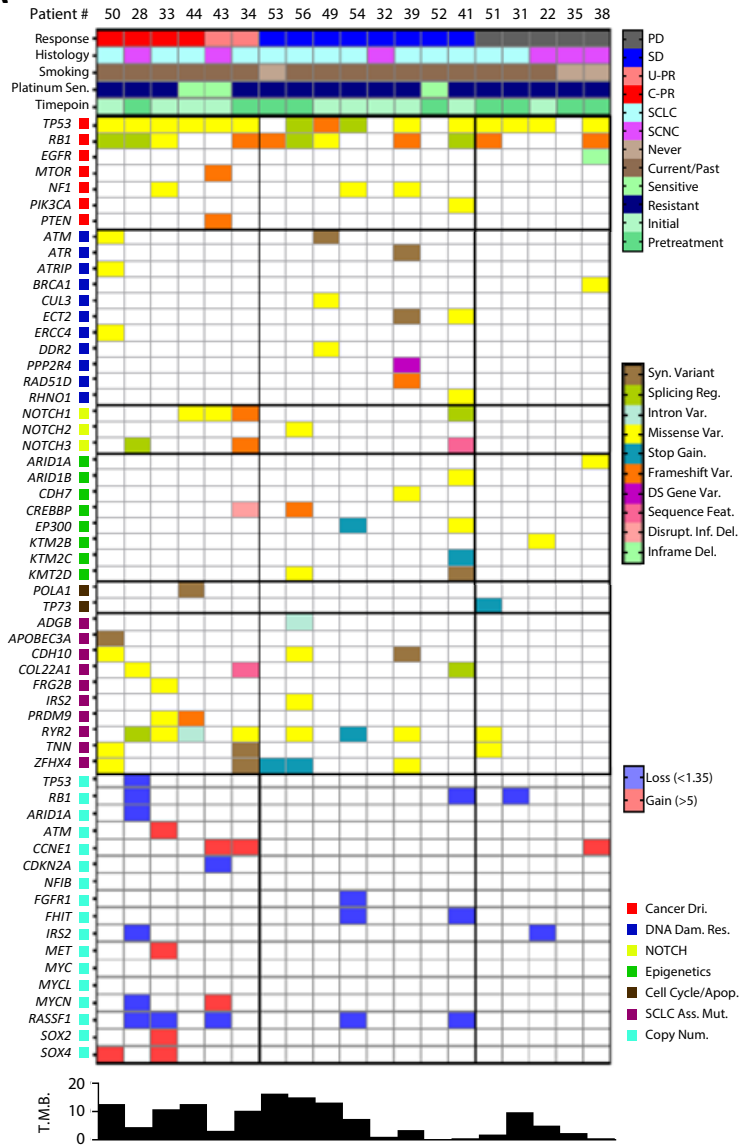


**Figure S3: Pharmacokinetics and efficacy of the combination of topotecan and M6620 in patients with SCLC, related to Figure 3.** **A)** Pharmacokinetics of topotecan in humans following intravenous administration (1.25 mg/m<sup>2</sup>) co-administered with M6620 with data separated by sex (6 males and 7 females). **B)** Pharmacokinetics of M6620 in humans following intravenous administration (210 mg/m<sup>2</sup>) co-administered with topotecan with data separated by sex (6 males and 6 females). **C)** Key PK parameters. Kaplan-Meier curves showing **D)** progression-free survival and **E)** overall survival in the overall trial population. **F)** Best response according to platinum sensitivity. **G)** Kaplan-Meier curve showing duration of response. Kaplan-Meier curves showing **H)** duration of response **I)** overall survival and **J)** progression-free survival in platinum-sensitive and resistant patients. **K)** progression-free survival and **L)** overall survival in patients who were previously treated with immunotherapy versus those who were not. **M)** Dose reductions, tumor response and duration of treatment.

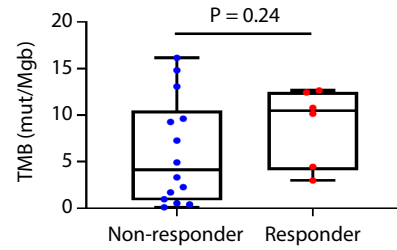


**Figure S4**

**A**



**B**



**C**

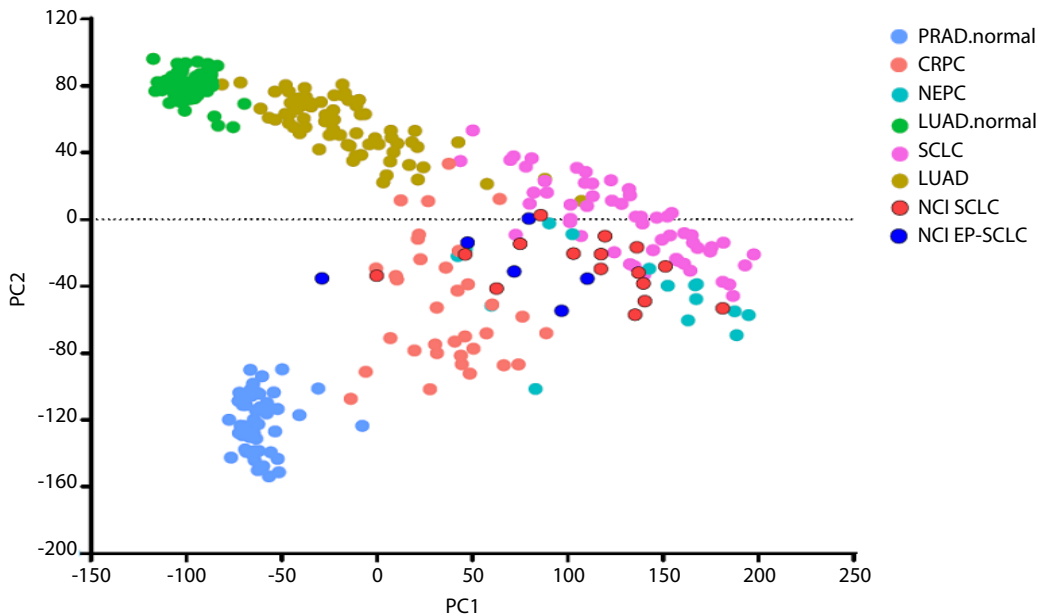
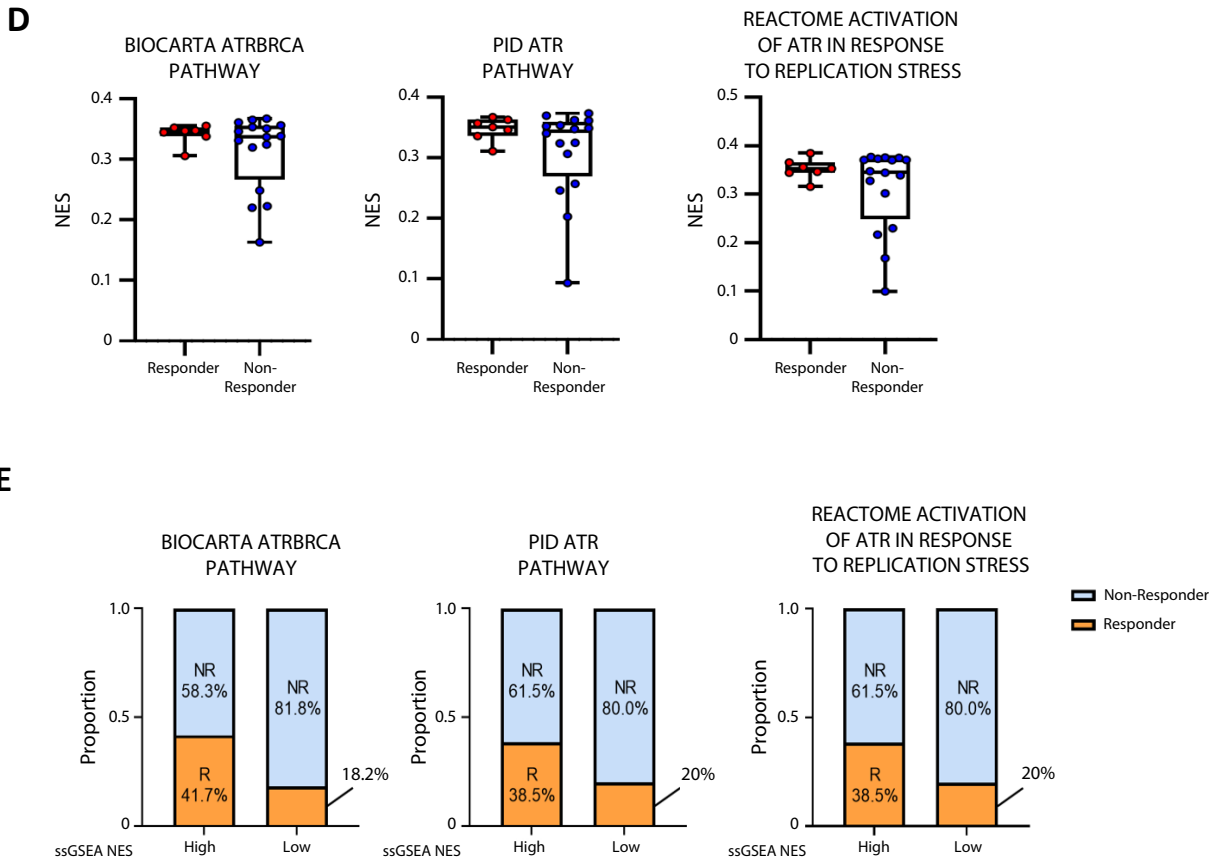
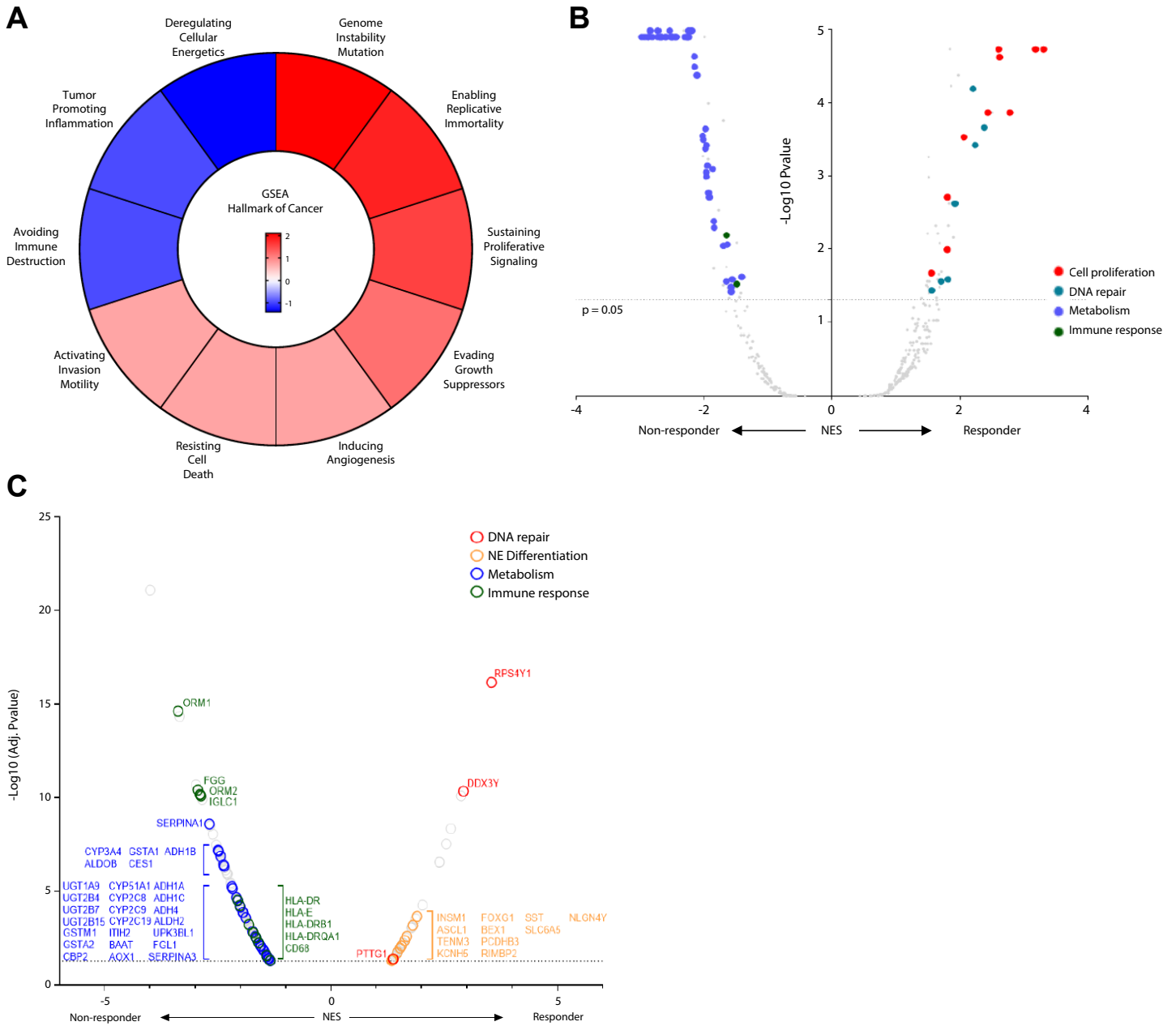


Figure S4 (cont.)



**Figure S4: Tumor exome, transcriptome, and replication stress signatures in responders and non-responders, related to Figure 5. A)** Mutations classified by type (e.g. intron variant, missense variant) and pathway (e.g. NOTCH signaling, epigenetics), and copy number variations among responders and non-responders. **B)** Boxplot showing the mutational burden of responders and non-responders (mut/Mb: mutations per megabase). **C)** Transcriptomic relationship of current cohort and previously published SCLC, lung adenocarcinoma, and prostate cancer cohorts. PRAD, prostate adenocarcinoma; CRPC, castration-resistant prostate cancer; NEPC, neuroendocrine prostate cancer; SCLC, small cell lung cancer; LUAD, lung adenocarcinoma; NCI SCLC and NCI EP-SCNC are samples from the current study. **D)** Box plot analysis of enrichment (NES) for selected ATR and replication stress-associated transcriptional signatures among responders and non-responders. **E)** Proportional analysis of responders and non-responders based on selected ATR and replication stress-associated transcriptional signatures.

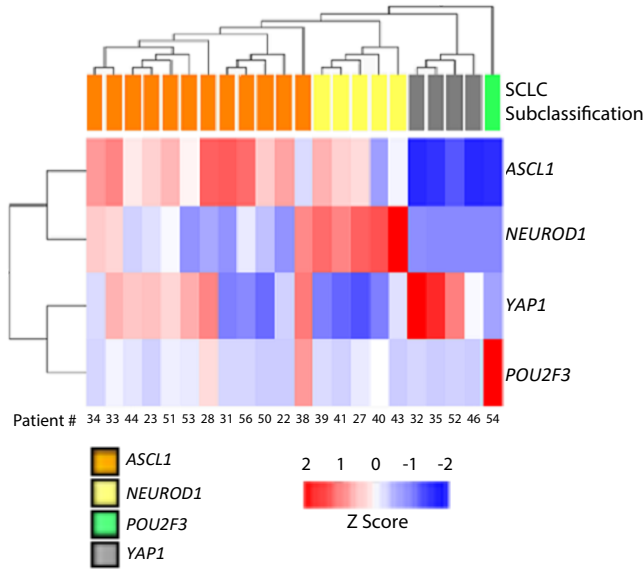
**Figure S5**



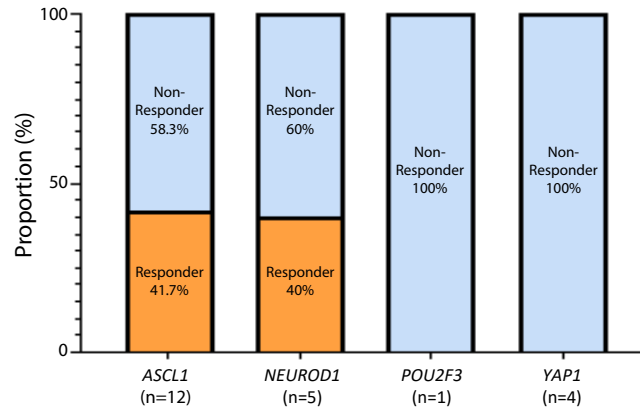
**Figure S5: Cancer hallmarks, genes, and gene sets differentially enriched among responders, related to Figure 5. A)** GSEA of cancer hallmarks based on differentially expressing genes between non-responders to M6620 and topotecan. **B)** Volcano plot showing gene set enrichments among SCLC responders and non-responders to M6620 and topotecan. Selected gene sets related to cell proliferation, DNA damage and replication, metabolism, and immune response are highlighted. **C)** Volcano plot showing differentially expressed genes between SCNC responders and non-responders to M6620 and topotecan. Selected genes related to DNA/RNA synthesis, metabolism, immune response and NE differentiation are highlighted.

**Figure S6**

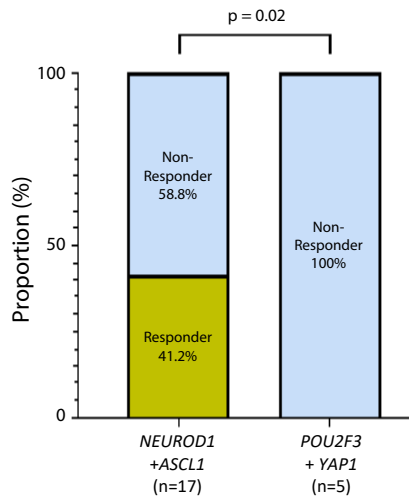
**A**



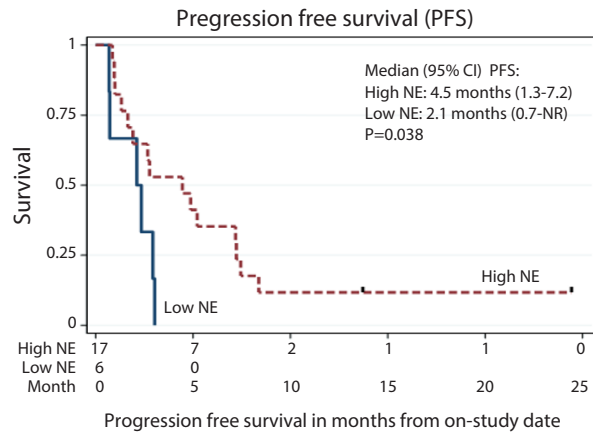
**B**



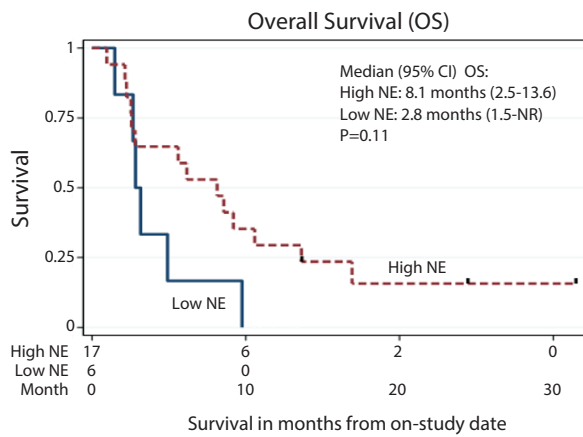
**C**



**D**



**E**



**F**

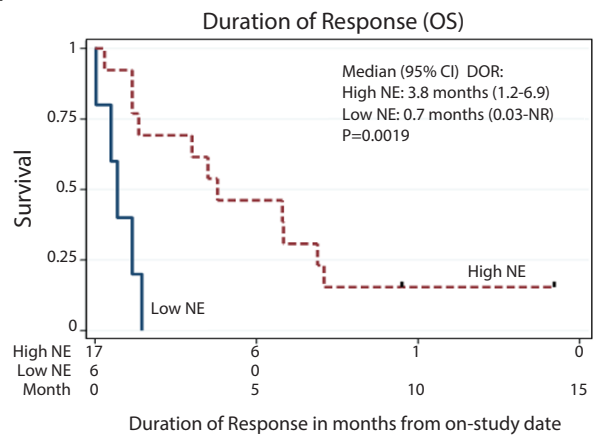


**Figure S6: SCNC transcriptional subtypes and response to M6620 and topotecan, related to Figure 5. A)** Hierarchical clustering of pre-treatment tumor transcriptomes based on expression of ASCL1, NEUROD1, YAP1 and POU2F3. **B and C)** Proportion of responses among SCNCs classified as ASCL1, NEUROD1, YAP1 and POU2F3. Kaplan-Meier curves showing **D)** progression-free survival and **E)** overall survival and **F)** duration of response based on high and low neuroendocrine signatures.